

Predictive Crystallization of Ribonuclease A via Rapid Screening of Osmotic Second Virial Coefficients

Peter M. Tessier,¹ Harvey R. Johnson,¹ Rajesh Pazhianur,¹ Bryan W. Berger,¹ Jessica L. Prentice,¹ Brian J. Bahnson,² Stanley I. Sandler,¹ and Abraham M. Lenhoff^{1*}

¹Center for Molecular and Engineering Thermodynamics, Department of Chemical Engineering, University of Delaware, Newark, Delaware

²Department of Chemistry and Biochemistry, University of Delaware, Newark, Delaware

ABSTRACT Important progress has been made in recent years toward developing a molecular-level understanding of protein phase behavior in terms of the osmotic second virial coefficient, a thermodynamic parameter that characterizes pairwise protein interactions. Yet there has been little practical application of this knowledge to the field of protein crystallization, largely because of the difficult and time-consuming nature of traditional techniques for characterizing protein interactions. Self-interaction chromatography has recently been proposed as a highly efficient method for measuring the osmotic second virial coefficient. The utility of the technique is examined in this work by characterizing virial coefficients for ribonuclease A under 59 solution conditions using several crystallization additives, including PEG, sodium chloride, ammonium sulfate, and propanol. The virial coefficient measurements show some counterintuitive trends and shed light on the previous difficulties in crystallizing ribonuclease A. Crystallization experiments at the corresponding solution conditions were conducted by using ultracentrifugal crystallization. Using this methodology, ribonuclease A crystals were obtained under conditions for which the virial coefficients fell within the “crystallization slot.” Crystallographic characterization showed that the crystals diffract to high resolution. Metastable crystals were also obtained for conditions outside, but near, the “crystallization slot,” and they could also be frozen and used to collect structural information. *Proteins* 2003;50:303–311. © 2002 Wiley-Liss, Inc.

Key words: protein interactions; self-interaction chromatography; static light scattering; ultracentrifugal crystallization

INTRODUCTION

Protein structural information obtained by X-ray diffraction of protein crystals has been instrumental in elucidating protein function^{1,2} and rationally designing medicinal drugs.^{3–5} However, obtaining protein crystals continues to be the most difficult step in the crystallographic determination of protein structure. There are numerous independent variables to adjust in attempting to obtain protein crystals, including the solvent conditions (pH, ionic strength, salt type, temperature, etc.) and protein concentration.

The large number of parameters and the unique crystallization behavior of each protein have led to the extensive use of empirical crystallization screens, which have the significant disadvantage of returning little information when they fail, which is often the case.

George and Wilson⁶ observed almost a decade ago that the osmotic second virial coefficient, a thermodynamic parameter that characterizes pairwise interactions between protein molecules in solution, correlated with solution conditions conducive to crystallization. Specifically, they found that the second virial coefficient values for nine proteins measured at their published crystallization conditions fell within a relatively narrow range of slightly negative, or weakly attractive, virial coefficient values. This range of virial coefficients, between -1 and -8×10^{-4} mol-mL/g², was named the “crystallization slot,” and its connection to the crystallization of several model proteins has been studied in detail.^{7–12} These studies suggested that this correlation may have potential for the rational determination of crystallization conditions for proteins that have not been crystallized previously. However, this approach has found little application as a predictive method in crystallization practice, largely because traditional methods for measuring virial coefficients, such as static light scattering and membrane osmometry, are experimentally complex and consume large amounts of protein.

We recently developed a faster, more efficient method for quantitatively measuring protein interactions by using a relatively new technique called self-interaction chromatography (SIC).^{13,14} The basis for SIC is that protein is

Grant sponsor: National Science Foundation; Grant numbers: BES-9510420 and BES-0078844; Grant sponsor: National Aeronautics and Space Administration; Grant number: NGT5-50167; Grant sponsor: National Institutes of Health Chemistry-Biology Interface Training Grant; Grant number: T32GM-08550.

H.R. Johnson's present address is College of Chemistry, University of California, Berkeley, CA 94720.

R. Pazhianur's present address is Rhodia Inc., CN 7500, 259 Prospect Plains Rd., Cranbury, NJ 08512.

*Correspondence to: Abraham M. Lenhoff, Center for Molecular and Engineering Thermodynamics, Department of Chemical Engineering, University of Delaware, Newark, DE 19716.

E-mail: lenhoff@che.udel.edu

Received 11 March 2002; Accepted 16 July 2002

TABLE I. Summary of Solution Conditions Used to Crystallize Ribonuclease A and the Corresponding Diffraction Parameters Obtained From Previous Studies and From This Work

Solution conditions	pH	Res. (Å)	Space group	Reference
30% tertiary butanol	5	1.1	P2 ₁	20
43% ethanol	5.3	2	P2 ₁	21
47% n-propanol	4–7	4	P6 ₂ 22	22
50% isopropanol	4–7	1.1–1.5	P2 ₁	22
60% methanol	~5	2.8	P2 ₁ 2 ₁ 2 ₁	23
70% 1,3-propanediol	7.1	1.8	C222 ₁	22
55% 2-methyl-2,4-pentanediol, 3.7 mM nickel chloride	6.4	1.5	P2 ₁ 2 ₁ 2 ₁	24
55% 2-methyl-2,4-pentanediol, 1:1 mol RNase A:Cu ²⁺	5.5	2.7	C2	23
55% 2-methyl-2,4-pentanediol, 1:1 mol RNase A:Ni ²⁺	6.1	2.8	P2 ₁	23
75% 2-methyl-2,4-pentanediol	9.5	1.8	P2 ₁ 2 ₁ 2 ₁	23
16% PEG 4000	-	2.3	P2 ₁ 2 ₁ 2 ₁	25
3 M cesium chloride, 1.8 M ammonium sulfate, 0.1 M triethanolamine	8.9	2.8	P3 ₂ 21	26
3 M sodium chloride, 1.8 M ammonium sulfate, 0.1 M sodium acetate	5.5	1.9	P3 ₂ 21	27
2.5 M sodium chloride, 3.3 M sodium formate, 0.1 M sodium acetate	5.5	1.9	P3 ₂ 21	27
3 M sodium chloride, 0.2 M ammonium sulfate, 20% xylitol	4	1.5	C2	Present work

immobilized on chromatographic particles that are packed into a column, and a pulse of the same protein is passed through the column. The relative retention of the protein pulse provides a measure of the average protein–protein interactions, which is related to the osmotic second virial coefficient.¹⁴ A significant advantage of this method over light scattering is that SIC requires at least an order of magnitude less time and protein.

The efficiency of SIC makes it possible to use second virial coefficient measurements to screen for suitable crystallization conditions. However, it does not provide an indication of the initial protein concentration for use in crystallization. Although it has been shown that a general correlation exists between the osmotic second virial coefficient and protein solubility for several globular proteins,^{10,15} the correlation is not strong enough to use as a predictive tool. In this work, we use ultracentrifugal crystallization^{9,16–19} to eliminate the need for solubility information to set the initial protein concentration properly. A dilute protein solution is placed in a high centrifugal field, which causes a steep concentration gradient at the bottom of the vial, resulting in nucleation. Nucleation depletes the protein concentration locally around the crystals, but protein continues to be delivered to the growing crystals by sedimentation. A significant advantage of this method is the resulting high initial and low subsequent protein concentrations, which are optimal for nucleation and growth, respectively. Ultracentrifugal crystallization also maintains constant solvent conditions during the crystallization procedure, which enables phase behavior measurements to be compared directly with virial coefficient measurements. Finally, the centrifugal concentration of protein can result in rapid crystal growth (crystals may appear within hours to days) relative to other common crystallization techniques, such as batch or vapor diffusion, which can take weeks to months to produce crystals.

In this article, we use SIC as a rapid screening tool to identify suitable solvent conditions for the crystallization of ribonuclease A (RNase A) and ultracentrifugal crystalli-

zation to confirm that crystals are indeed obtained. Our investigation of virial coefficient trends for RNase A, including the effects of pH, ionic strength, and several additives, represents the most extensive set of virial coefficient data available for a single protein, and thus presents a good test of the predictive capability of the George and Wilson⁶ “crystallization slot.” We chose RNase A as our model protein because the solution conditions that have been used historically to crystallize RNase A contain high concentrations of precipitants, often requiring the use of organic solvents (Table I). Herein we provide physical insight into RNase A interactions and conditions for rapid and high-quality crystallization. More generally, we illustrate a systematic and efficient method for obtaining protein crystals that we believe can be readily applied to other proteins.

MATERIALS AND METHODS

Materials

RNase A (R-5503) was obtained from Sigma and used as received. Citric acid (ACS grade, C-1909), bis-tris (B-7535), 25% glutaraldehyde (G-5882), polyethylene glycol (MW 3350, P-4338), xylitol (X-3375), and ethanolamine (E-9508) were also purchased from Sigma. Potassium phosphate (ACS grade, P288), hydrochloric acid (ACS grade, A114), ammonium sulfate (ACS grade, A702), sodium carbonate (ACS grade, S263), and sodium chloride (ACS grade, 5271) were purchased from Fisher. Glacial acetic acid was obtained from Mallinckrodt (3121). Tris (819620) was obtained from ICN. Propanol (29,328-8) was purchased from Aldrich. Micro-BCA assay reagents (23231BP, 23232BP, and 23234BP) were obtained from Pierce. AF-Amino-650M chromatography particles (08002) were obtained from Tosoh Biosep (formerly TosoHaas). All protein solutions and buffers were prepared with distilled water that was further purified by using a Millipore Milli-Q system (>18.2 MΩ-cm). The pH was adjusted by using hydrochloric acid or sodium hydroxide and measured by using a Chemcadet 5984 digital pH meter.

For SIC, electrolyte solutions without protein were filtered through 220-nm Gelman bottle top filters (4632) into 2-L Corning sterile roller bottles (431133) and stored at room temperature. RNase A solutions were filtered through 220-nm Millipore Millex-GV syringe filters (SLGVR25LS) before use. The concentration of RNase A was determined using a Perkin-Elmer Lambda 4B spectrophotometer at 280 nm, using an extinction coefficient of 0.70 L/g-cm.²⁸ All experiments were carried out at room temperature (23 ± 2°C).

Methods and Theory

Self-interaction chromatography

SIC measurements of second virial coefficients were conducted using a modification of the procedure reported previously.¹⁴

Protein immobilization. RNase A was immobilized on Tosoh Biosep AF-Amino-650M particles by using glutaraldehyde to link primary amine groups, of which there are 10 per molecule, on the protein surface to primary amine groups on the particle surface.²⁹ Two milliliters of particles were washed with 1 L of water and were combined with 2 mL of 0.4 M sodium carbonate buffer at pH 10 and 2 mL of 25% glutaraldehyde. The activation reaction was allowed to proceed overnight, and the glutaraldehyde was then removed by washing the particles on a glass frit with >2 L of water. Thorough removal of the free glutaraldehyde was critical because it readily cross-links protein in solution. Furthermore, the absorbance maximum for glutaraldehyde is at ~280 nm, which will interfere with the UV measurements of the unbound protein in the wash solutions that are used to determine the amount of protein bound.³⁰

After the glutaraldehyde was removed, the particles were added to ~55 mg of RNase A that was dissolved in 11 mL of 1 M potassium phosphate at pH 8.5. The solution was allowed to react overnight, and the particles were then washed with ~250 mL of 1 M potassium phosphate solution at pH 8.5. The particles were added to a solution of 1 M ethanolamine at pH 8 to block any unreacted glutaraldehyde on the particle surface. After a few hours, the particles were washed with 250 mL of the same phosphate buffer and stored at neutral pH. The amount of protein immobilized was analyzed by absorbance measurements at 280 nm of the initial and wash solutions, and by the micro-BCA method using the particles with immobilized protein.^{14,31} Both analysis methods gave an immobilization density of ~15 mg of RNase A per milliliter of settled particles, or a surface coverage of ~35%, which was found previously to be optimal for lysozyme virial coefficient measurements.¹⁴

Chromatography procedure and data analysis. An automated Pharmacia FPLC system was used to conduct the chromatography experiments and to analyze the results. The particles were packed into a 1-mL Waters AP glass minicolumn (5 × 50 mm) at a flow rate of 3 mL/min until the bed height remained stable. RNase A samples were prepared at 5 mg/mL at a variety of solution conditions. Once the column had been equilibrated with

the eluent of the composition of interest for 10 column volumes at 0.75 mL/min, the flow rate was reduced to 0.4 mL/min, and 50 µL of the sample was injected into the column. After the peak had eluted, the flow rate was again increased to 0.75 mL/min, and the column was washed with a high salt buffer (typically 1 M sodium chloride) for three column volumes, and then with a low ionic strength buffer for about seven column volumes. The procedure was then repeated at the solution conditions of the next sample. Samples were typically run in triplicate to ensure reproducible results. Because the peaks were usually symmetric, the peak maximum was used to determine the retention volume.

We characterized the chromatographic retention in terms of the retention factor,

$$k' = \frac{V_r - V_o}{V_o} \quad (1)$$

where V_r is the retention volume, or the volume required to elute a solute from the column, and V_o is the dead volume, or the volume required to elute a noninteracting solute of the same size from the same column. A column packed with the same particles without protein immobilized was used to determine V_o .¹⁴

If proteins in solution interact with a randomly oriented partial monolayer of immobilized protein, the second virial coefficient can be related to the retention factor by¹⁴

$$B_{22} = B_{HS} - \frac{k'}{\rho_s \phi} \quad (2)$$

where B_{HS} is the excluded volume or hard sphere contribution ($B_{HS} = 4v_m$ for spheres, where v_m is the molecular volume), ρ_s is the amount of protein immobilized per unit surface area, and ϕ is the phase ratio, or the available surface area per mobile phase volume, which is available for a variety of chromatography particles.³² The molecular volume can be calculated by using the Molecular Surface Package.^{33,34}

Ultracentrifugal crystallization

Centrifugal crystallization was carried out in a Sorvall Discovery 90 ultracentrifuge with a Beckman SW5 1-50,000 RPM rotor and Beckman centrifuge tubes (344057). Forty milligrams of RNase A in 4 mL of solution was used for each sample, and the samples were centrifuged for 48 h at 45,000 rpm. After the centrifugation was complete, most (~80%) of the supernatant was removed, and the solutions were examined by optical microscopy. The samples were then stored at 4°C to determine if any further phase separation would occur.

On the basis of our previous experiments with catalase¹⁷ and chymotrypsinogen,⁹ we performed centrifugation runs at a speed that would permit complete sedimentation of the protein in 48 h. This speed was calculated on the basis of the sedimentation velocity with a sedimentation coefficient of 1.78×10^{-13} sec,³⁵ which was corrected for the solvent density. The centrifugal speed based on these calculations was ~45,000 rpm.

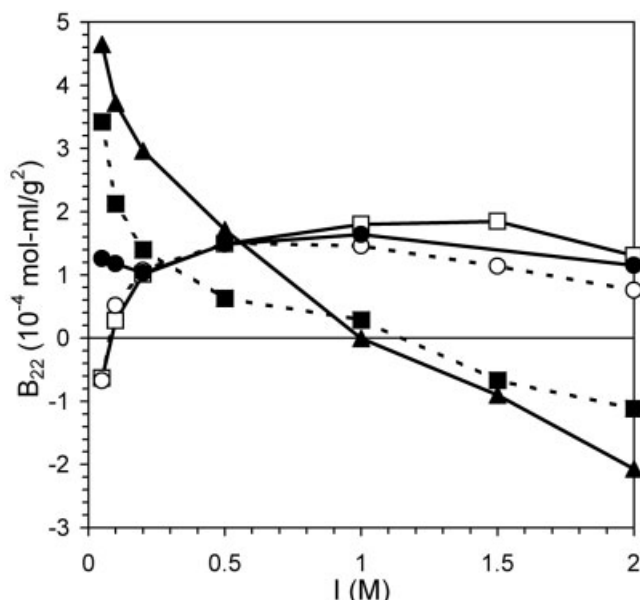


Fig. 1. Ribonuclease A virial coefficients measured by self-interaction chromatography as a function of sodium chloride ionic strength at pH 3 (▲), pH 4 (■), pH 5 (●), pH 6.5 (□), and pH 8 (○).

X-ray diffraction analysis

X-ray diffraction data were collected by using a Rigaku RU300 rotating anode generator with a RAXIS IV image plate area detector. The crystals used were grown in a solution containing the crystallization agents and the cryoprotectant (20 wt % xylitol). Immediately after the removal of the crystals from the ultracentrifuge, the crystals were selected with a 0.3-mm loop and flash frozen in liquid nitrogen (-180°C). The programs DENZO and SCALEPAK were used for crystallographic indexing, data processing, and scaling.³⁶

RESULTS AND DISCUSSION

Self-Interaction Chromatography

We used SIC to explore a wide range of solution conditions ranging from pH 3 to 8, ionic strengths up to 4 M, and additives such as PEG and n-propanol. Figure 1 shows a summary of virial coefficients measured by SIC in sodium chloride from pH 3–8. At pH 3 and 4, the virial coefficients indicate repulsive interactions at low ionic strength and attractive interactions at high ionic strength. The interactions at high salt concentrations (>1 M sodium chloride) are most attractive at low pH, that is, farthest from the isoelectric point (RNase $\text{pI} = 9.6$).³⁷ At pH 5 and low ionic strength, a decrease in the repulsive interactions as a function of salt concentration is also observed, similar to that observed at pH 3 and 4, although this change in the virial coefficient values is only slightly larger than the average standard deviation of our SIC experiments (0.3×10^{-4} mol·ml/ g^2). The virial coefficient trend at pH 5 reverses at >0.2 M sodium chloride, and the interactions become more repulsive, instead of more attractive. At pH 6.5 and 8, the virial coefficient trends are completely reversed, and the interactions are attractive at low ionic

strength and repulsive at high ionic strength. Nonspecific interactions between free RNase A molecules in solution and the particle surface were confirmed to be negligible because the retention of RNase A changed by only 1% between pH 3 and 6.5 at 0.8 M sodium chloride with an identical column without immobilized protein.

The surprising dependence of the virial coefficient values on pH at high salt concentration (>1 M sodium chloride) may be caused by changes in hydration of RNase A. It has been shown that the most hydrated amino acids are the acidic residues Asp and Glu and that the hydration of these amino acids depends strongly on their protonation state.³⁸ RNase A has 10 Glu and Asp residues, which have pK_a values of ~ 4.6 .³⁷ Therefore, at pH 3 and 4, the acidic residues are weakly hydrated, whereas at pH 5, 6.5, and 8, the acidic residues have at least 3 times more water bound.³⁸ The increase in the number of bound water molecules at pH values > 5 may hinder the association of RNase A molecules in configurations that are energetically favorable, such as crystal contacts. There are multiple acidic residues located at the dimer interface and at the crystal contacts of RNase A crystals grown in a high salt environment,²⁰ indicating that hydration may play an important role in RNase A interactions.

The pronounced change in virial coefficient trends at low ionic strength between pH 5 and 6.5 may be explained by examining the net charge³⁷ and the charge distribution³⁹ of RNase A shown in Figure 2. Figure 2(A) shows that between pH 5 and 6.5, the net charge of RNase A is reduced from approximately +8 to +4, which would increase the importance of the spatial charge distribution shown in Figure 2(B). It can be seen in this figure, in which Glu and Asp residues are in red and Lys and Arg residues are in blue, that the charge distribution is highly anisotropic, with isolated patches of positive and negative charge observable. Therefore, attractive interactions between oppositely charged patches may contribute significantly to the overall change in the measured virial coefficients from pH 5 to 6.5 at low ionic strength, which is in qualitative agreement with previous molecular-level calculations for α -chymotrypsinogen interactions.⁴⁰

It also is interesting that almost all of the virial coefficients measured from pH 4 to 8 and between 0 and 2 M sodium chloride lie above the "crystallization slot" (-1 to -8×10^{-4} mol·ml/ g^2), which provides some insight into why RNase A is so difficult to crystallize. Because virial coefficient values at low pH and high salt concentration are closest to the "crystallization slot," we explored the effect of increasing the ionic strength beyond 2 M by using sodium chloride and ammonium sulfate; the results are shown in Figure 3. High concentrations of sodium chloride (>1 M) resulted in more attractive interactions than for ammonium sulfate, which was also observed previously for lysozyme ($\text{pI} 11$), another basic protein, directly in terms of virial coefficients⁴¹ and indirectly in terms of solubility measurements.⁴² Although sulfate is expected to be a better precipitant than chloride because of its high ranking in the Hofmeister series,⁴³ the original precipitation studies by Hofmeister were conducted at neutral pH using

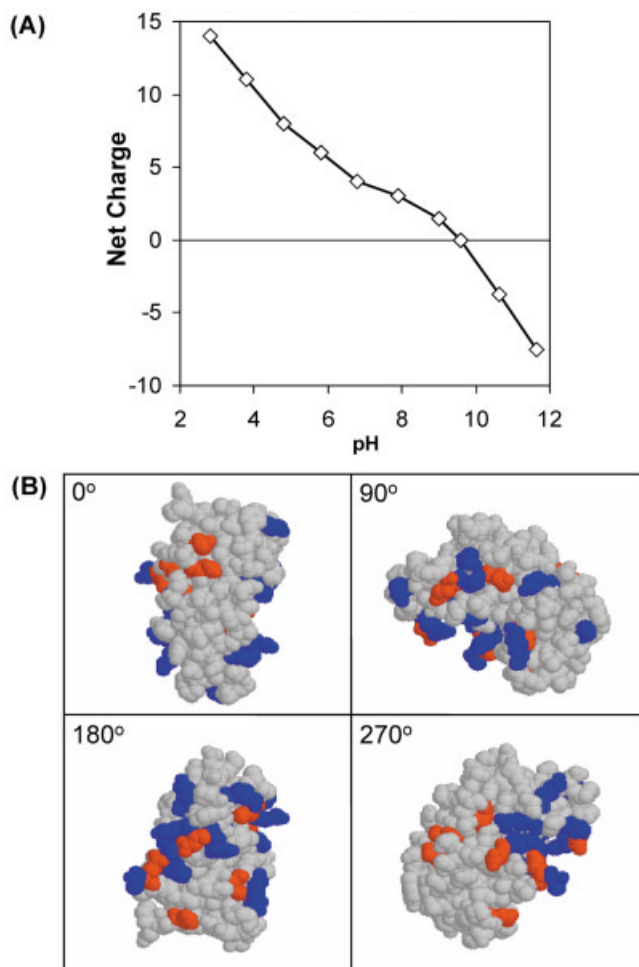


Fig. 2. **A:** Net charge of ribonuclease A as a function of pH from Tanford and Hauenstein.³⁷ **B:** Spatial distribution of charge for ribonuclease A viewed by rotation around the y axis. Acidic residues aspartic and glutamic acid are shown in red, and basic residues lysine and arginine are shown in blue.

egg white, which consists primarily of the acidic protein ovalbumin (pI 4.6). More recently it was confirmed that the order of the Hofmeister series depends on the charge of the protein; the normal Hofmeister series is observed at pH values above the pI of the protein,⁴⁴ whereas the opposite trend is observed at pH values below the pI of the protein.⁴²

At or above an ionic strength of 3 M, both electrolytes caused the virial coefficient measurements to fall within the "crystallization slot." A mixture of 0.2 M ammonium sulfate and 3 M sodium chloride, which are conditions reported previously to crystallize RNase A at pH 5,⁴⁵ gave a virial coefficient intermediate to that of sodium chloride and ammonium sulfate at a corresponding ionic strength, as expected. We also measured the virial coefficient for this mixture of ammonium sulfate and sodium chloride in the presence of 20 wt % xylitol because we attempted to crystallize RNase A in the presence of xylitol as a cryoprotectant. The virial coefficient measured in the presence of xylitol was -4.0 compared to $-4.2 \times 10^{-4} \text{ mol-mL/g}^2$ in

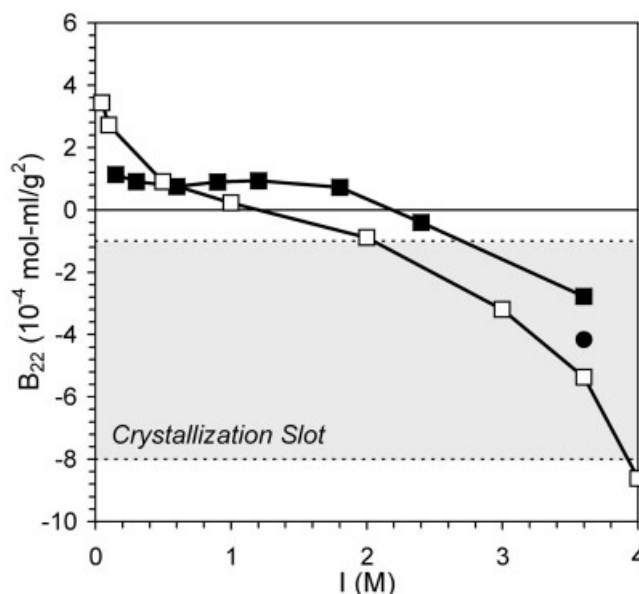


Fig. 3. Ribonuclease A virial coefficients measured by self-interaction chromatography at pH 4 in sodium chloride (\square), ammonium sulfate (\blacksquare), and a 15 to 1 molar mixture of sodium chloride and ammonium sulfate (\bullet).

the absence of xylitol. Xylitol caused the protein interactions to be less attractive, which is expected because xylitol is used as an excipient in protein formulation, although this change is minor. We also tested the reproducibility of the SIC column over time and found that the virial coefficient measurements changed by an average of $0.2 \times 10^{-4} \text{ mol-mL/g}^2$ over 6 weeks, indicating that the same column can be used to make reproducible measurements for more than a month.

Boyer et al.⁴⁵ characterized RNase A interactions using dynamic light scattering by measuring the increase (repulsion) or decrease (attraction) in the RNase A diffusion coefficient as a function of protein concentration at various solution conditions. At low ionic strength (50 mM acetate), they observed repulsive interactions at pH 4 and 5, whereas the interactions became attractive at pH 6.5 and 8, in agreement with our observations. Furthermore, at high ionic strength (3 M sodium chloride and 0.2 M ammonium sulfate), they also observed that decreasing pH resulted in more attractive interactions.

An important difference, however, between our measurements by SIC and those of Boyer et al.⁴⁵ is that dynamic light scattering measurements do not allow direct thermodynamic information to be extracted, because the measurements are affected by hydrodynamic forces as well.⁴⁶ The advantage of the virial coefficient is that thermodynamic information is obtained directly and may be used for predictive crystallization. Although efforts are being made to develop a correlation between dynamic light scattering measurements and the "crystallization slot,"⁴⁷ we believe that the virial coefficient is a more desirable quantity because it has a clear connection to the potential of mean force, which characterizes the pairwise interaction energy.

The significant use of organic solvents to crystallize RNase A (Table I) led us to study the effect of n-propanol

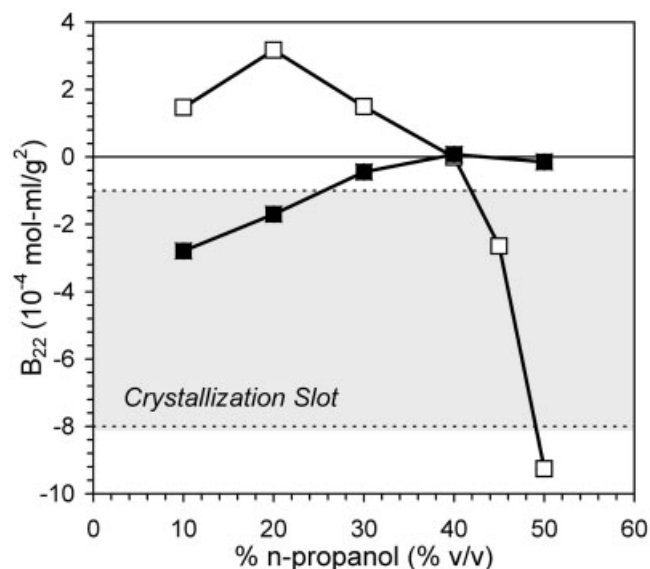


Fig. 4. Ribonuclease A virial coefficients measured by self-interaction chromatography in propanol at pH 5 (□) and pH 8 (■).

on the second virial coefficient. Figure 4 shows that RNase A interactions in propanol depend significantly on pH. At pH 5 and low propanol concentrations, the interactions became more repulsive with initial increases in propanol concentration. However, as the propanol concentration was increased further, the interactions became attractive, and the virial coefficient values fell within the "crystallization slot." The opposite trend was observed at pH 8; at low propanol concentrations, the interactions were attractive, whereas at high propanol concentrations, the virial coefficients were approximately zero.

The effect of polyethylene glycol (PEG, 3350 MW) was also explored. Because RNase A virial coefficients at pH 8 and low ionic strength were close to the "crystallization slot," virial coefficient measurements were conducted at pH 8 and 0.05 M sodium chloride in the presence of PEG to determine whether PEG-induced depletion interactions could reduce the virial coefficient to values within the "crystallization slot." The measurement of virial coefficients in the presence of PEG required two modifications of SIC. First, the interaction measurements depend on injection concentration because the peaks obtained were highly asymmetric at low injection concentrations (e.g., 5 mg/mL) and high PEG concentrations (>8 wt %). However, above a concentration of 20 mg/mL, the SIC measurements became independent of injection concentration, and the peaks were more symmetric at PEG concentrations up to 15 wt %. Therefore, to measure virial coefficients in the presence of PEG, we used an injection concentration of 25 mg/mL of RNase A for all concentrations of PEG versus an injection concentration of 5 mg/mL for all other crystallization agents because the virial coefficient measurements were independent of injection concentration. Although the origin of the dependence of peak shape on injection concentration is unclear, similar behavior has also been observed for lysozyme in sodium chloride solutions.¹⁴ In a previous

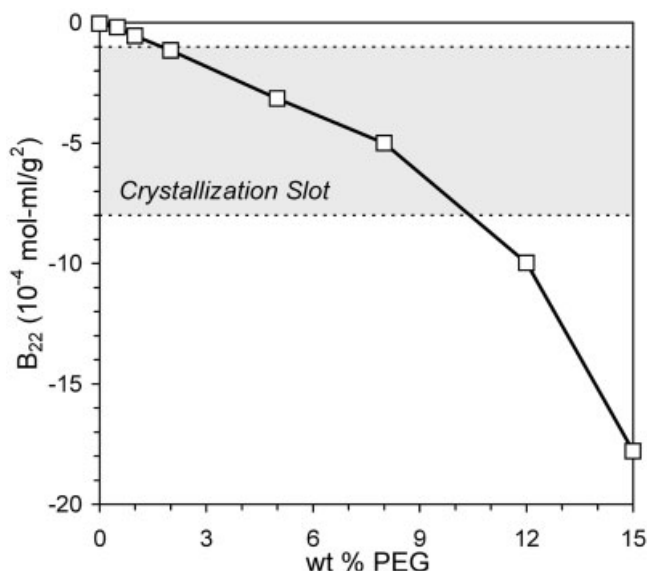


Fig. 5. Ribonuclease A virial coefficients measured by self-interaction chromatography at pH 8 and 50 mM sodium chloride at various concentrations of polyethylene glycol (MW 3350).

study, it was shown that the dependence of peak shape and peak position on injection concentration was strongly linked to the surface coverage of immobilized protein. It was speculated that the behavior was due to free lysozyme molecules interacting simultaneously with more than one immobilized molecule. It is possible that because of depletion effects in the presence of PEG, free RNase A molecules are forced between immobilized proteins, increasing the likelihood of free proteins simultaneously interacting with multiple immobilized proteins. It is also interesting that for both the lysozyme and RNase A measurements, the surface coverage, protein size, and the injection concentration at which the SIC measurements became independent of injection concentration were nearly identical.

The other modification of SIC necessary to measure RNase A interactions in the presence of PEG was that the flow rate through the column was reduced proportionally to the increase in the viscosity of the PEG solution relative to that of water. For chromatographic peaks to be symmetric, it is important to use a flow rate low enough to allow solute diffusion into the particles during the solute transit through the column. Because the diffusivity is inversely related to the solvent viscosity, increasing the PEG concentration decreases the rate of diffusion. Therefore, we scaled the flow rate by the viscosity of the PEG solution relative to water to maintain roughly an equal rate of diffusion and, more importantly, to obtain peaks that were reasonably symmetric. As shown in Figure 5, the virial coefficient became significantly more attractive in the presence of PEG, and several solution conditions were found to lie within the "crystallization slot."

An important limitation of static light scattering, which is the most commonly used method to measure virial coefficients, is that scattering from large crystallization agents (e.g., PEG) at high concentrations can become

TABLE II. Summary of Virial Coefficient Measurements for Ribonuclease A and the Corresponding Phase Behavior Determined Largely by Ultracentrifugal Crystallization

pH	Crystallization additives	Phase separation	B_{22} (10^{-4} mol·ml/g ²)
6.5	1 M sodium chloride	none	1.8
6.5	1.5 M sodium chloride	none	1.8
6.5	0.5 M sodium chloride	none	1.5
5	10 wt % propanol	none	1.5
5	30 wt % propanol	none	1.5
5	0.1 M sodium chloride	none	1.3
5	1 M sodium chloride	none	1.3
5	1 M sodium chloride	none	1.3
5	0.5 M sodium chloride	none	1.3
5	1.5 M sodium chloride	metastable crystal	1.2
5	2 M sodium chloride	metastable crystal	1.2
4	2 M sodium chloride	metastable crystal	-0.9
8	0.05 M sodium chloride	none	-0.9
5	45 wt % propanol	precipitate	-2.7
4	1.2 M ammonium sulfate	precipitate	-2.8
4	3 M sodium chloride	stable crystal	-3.2
4	1.0 M ammonium sulfate, 0.6 M sodium chloride, 20 wt % xylitol	stable crystal	-4.0
4	1.0 M ammonium sulfate, 0.6 M sodium chloride	stable crystal	-4.2
4	3.6 M sodium chloride	stable crystal	-5.4
4	4 M sodium chloride	stable crystal	-8.6
8	12 wt % PEG	precipitate	-10.0
8	15 wt % PEG	precipitate	-17.8

The precipitate phase behavior results at pH 8 were evaluated using batch crystallization. The location of the “crystallization slot” is denoted by the bold lines.

significant and complicate the interpretation of scattering results. Because the scattering from a two-component system is not a linear combination of the scattering of the individual components, it can be difficult to extract the scattering intensity because of protein–protein interactions from, for example, the protein-PEG or the PEG-PEG interactions. Kulkarni et al.^{48,49} argued that the contribution of the cross-scattering term due to the protein-PEG interactions is small at low polymer concentration (approximately <10 wt % for 6-kD PEG). Higher concentrations or higher molecular weights of PEG can complicate light-scattering measurements not only because of protein-PEG cross-interactions but also because of the relatively small contribution of scattering from the protein molecules relative to the large amount of scattering from the PEG molecules.

Ultracentrifugal Crystallization

To evaluate the predictive capability of the George and Wilson “crystallization slot,”⁶ RNase A phase behavior was explored by using ultracentrifugal crystallization, which has the distinct advantage of maintaining constant solution conditions (but not protein concentration) while crystallization proceeds when the additives are small and not affected by the centrifugal field. This is not the case for large polymers such as PEG (MW 3350), which were used in this work, and which did phase separate once concentrated at the bottom of the centrifuge tube. Therefore, we also conducted phase behavior experiments in the presence of PEG with use of batch crystallization by preparing

RNase A solutions at a fixed concentration (~30 mg/mL) and temperature (4°C) in a stagnant environment. At high PEG concentrations (>8 wt % PEG), these solutions phase separated over a period of several months.

We evaluated the phase behavior of RNase A for 21 of the 59 conditions at which virial coefficients were measured. The results in Table II show that the solution conditions that yielded either protein crystals or precipitates fall either within or below the “crystallization slot” (-1 to -8×10^{-4} mol·mL/g²), whereas the conditions that did not lead to stable phase separation generally lie above the “crystallization slot.” These results are consistent with the ideas of protein phase behavior presented by George and Wilson.⁶

It is not surprising that two solution conditions that correspond to virial coefficient values within the “crystallization slot” led to a precipitate rather than a crystalline phase because the second virial coefficient is a highly averaged measure of protein interactions, to which local interactions in specific pairwise configurations may contribute disproportionately.⁴⁰ Some solution conditions that lead to weakly attractive protein interactions globally may promote denaturation or specific interactions locally that interfere with the formation of crystal contacts, which could lead to a disordered precipitate. The precipitate condition inside the “crystallization slot” at pH 4 corresponds to 1.2 M ammonium sulfate. The cause of the precipitate phase may be related to sulfate binding to the positively charged residues,⁵⁰ which could interfere with the formation of crystal contacts or the dehydration of the

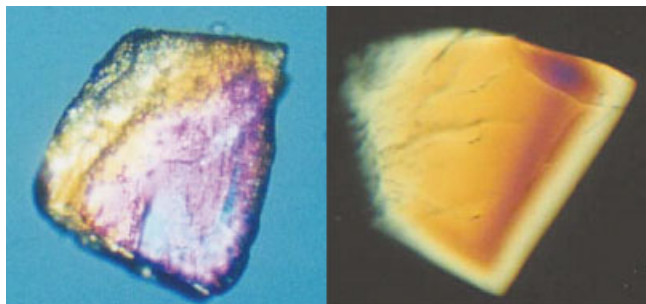


Fig. 6. Ribonuclease A crystals formed in 20 wt % xylitol at pH 5 and 2 M sodium chloride (A), and pH 4, 3 M sodium chloride and 0.2 M ammonium sulfate (B). The crystal on the left was metastable and would dissolve within 30 min after removal from the ultracentrifuge, whereas the crystal on the right was stable indefinitely. The size of the crystals is ~ 0.5 mm.

protein interface. The precipitate condition at pH 5 that falls within the "crystallization slot" corresponds to 45 vol % propanol, which is close to crystallization conditions reported previously for RNase A.²² However, only a broad range of pH 4 to 7 was reported in a previous study, whereas our results suggest that pH has a strong effect on RNase A interactions in propanol, which makes comparison of the crystallization conditions difficult. Although RNase A has been crystallized in several organic solvents, denaturation is still a concern and could lead to precipitation rather than crystallization.

Metastable crystals refer to crystals that formed in the centrifugal field but were not stable when removed from the ultracentrifuge. These crystals typically dissolved within 30 min, even after most of the supernatant was removed in an attempt to prevent the crystals from dissolving because of dilution at the bottom of the centrifuge tube by the supernatant. A comparison of a metastable crystal and a crystal that was stable indefinitely is shown in Figure 6. The metastable crystal, which was formed in 2 M sodium chloride and 20 wt % xylitol at pH 5, had irregular boundaries where dissolution was occurring [Fig. 6(A)], whereas the stable crystal, which was formed in 3 M sodium chloride, 0.2 M ammonium sulfate, and 20 wt % xylitol at pH 4, had sharp edges [Fig. 6(B)].

X-ray diffraction revealed that the space group of the RNase A crystals grown by ultracentrifugal crystallization was C2, and the cell dimensions were $a = 116.3$ Å, $b = 67.1$ Å, $c = 63.9$ Å and $\beta = 90.03^\circ$. Although other RNase A structures have been reported for the space group C2,²³ the cell dimensions reported in this work are different and thus represent a new crystal form. Although the resolution limit was higher for the stable crystals (1.5 Å) versus the metastable crystals (2.0 Å), it was still feasible to flash freeze the less stable form in liquid nitrogen and collect X-ray diffraction data in a nitrogen cryo stream at -180°C . The cryo conditions significantly extended the lifetime of the protein crystals and enabled the collection of useful data. The ability to trap crystals in a metastable state and collect structural data is particularly important because, at the end of an ultracentrifugal crystallization experiment, the steep protein concentration gradient is lost,

which can cause dissolution of the metastable protein crystals. Additional studies are necessary to confirm the generality of this finding.

CONCLUSIONS

We have shown that self-interaction chromatography can be used to measure protein interactions in terms of the second virial coefficient rapidly and efficiently and that this information can be used to rationally determine solution conditions under which RNase A will crystallize. Counterintuitive virial coefficient trends as a function of pH were found at both low and high ionic strength, confirming the importance of measuring protein interactions to understand crystallization behavior. Based on the virial coefficient information, ultracentrifugal crystallization was used to obtain high-quality crystals, and it was shown that metastable crystals could be frozen and also used to obtain structural information. The principal conclusion of this work is that self-interaction chromatography holds significant promise as a rapid screening method for crystallizing proteins and may be a particularly attractive tool for investigating proteins that are difficult to crystallize, such as membrane proteins.

ACKNOWLEDGMENTS

We are grateful for support from the National Science Foundation, National Aeronautics and Space Administration for a GSRP Fellowship to P.M.T., and National Institutes of Health for support of B.W.B. under a Chemistry-Biology Interface Training Grant.

REFERENCES

1. Moffat K. Time-resolved biochemical crystallography: a mechanistic perspective. *Chem Rev* 2001;101:1569–1581.
2. Lolis E, Petsko GA. Transition-state analogs in protein crystallography—probes of the structural source of enzyme catalysis. *Annu Rev Biochem* 1990;59:597–630.
3. Gane PJ, Dean PM. Recent advances in structure-based rational drug design. *Curr Opin Struct Biol* 2000;10:401–404.
4. Klebe G. Recent developments in structure-based drug design. *J Mol Med* 2000;78:269–281.
5. Amzel LM. Structure-based drug design. *Curr Opin Biotech* 1998;9:366–369.
6. George A, Wilson WW. Predicting protein crystallization from a dilute-solution property. *Acta Crystallogr D* 1994;50:361–365.
7. Bonneté F, Finet S, Tardieu A. Second virial coefficient: variations with lysozyme crystallization conditions. *J Cryst Growth* 1999;196:403–414.
8. Hitscherich C, Kaplan J, Allaman M, Wiencek J, Loll PJ. Static light scattering studies of OmpF porin: implications for integral membrane protein crystallization. *Protein Sci* 2000;9:1559–1566.
9. Pjura PE, Lenhoff AM, Leonard SA, Gittis AG. Protein crystallization by design: chymotrypsinogen without precipitants. *J Mol Biol* 2000;300:235–239.
10. Rosenbaum DF, Zukoski CF. Protein interactions and crystallization. *J Cryst Growth* 1996;169:752–758.
11. Tardieu A, Finet S, Bonneté F. Structure of the macromolecular solutions that generate crystals. *J Cryst Growth* 2001;232:1–9.
12. Vellev OD, Kaler EW, Lenhoff AM. Protein interactions in solution characterized by light and neutron scattering: comparison of lysozyme and chymotrypsinogen. *Biophys J* 1998;75:2682–2697.
13. Patro SY, Przybycien TM. Self-interaction chromatography: a tool for the study of protein-protein interactions in bioprocessing environments. *Biotechnol Bioeng* 1996;52:193–203.
14. Tessier PM, Lenhoff AM, Sandler SI. Rapid measurement of protein osmotic second virial coefficients by self-interaction chromatography. *Biophys J* 2002;82:1620–1631.

15. Guo B, Kao S, McDonald H, Asanov A, Combs LL, Wilson WW. Correlation of second virial coefficients and solubilities useful in protein crystal growth. *J Cryst Growth* 1999;196:424–433.
16. Wyckoff RWG, Corey RE. The ultracentrifugal crystallization of tobacco mosaic virus protein. *Science* 1936;84:513.
17. Karpukhina SY, Barynin VV, Lobanova GM. Crystallization of catalase in the ultracentrifuge. *Sov Phys Crystallogr* 1975;20:417–418.
18. Barynin VV, Melik-Adamyany VR. The mechanism of crystallization of proteins in an ultracentrifuge. *Sov Phys Crystallogr* 1982;27:588–591.
19. Lenhoff AM, Pjura PE, Dilmore JG, Godlewski TS. Ultracentrifugal crystallization of proteins: transport-kinetic modelling, and experimental behavior of catalase. *J Cryst Growth* 1997;180:113–126.
20. Svensson LA, Dill J, Sjolin L, Wlodawar A, Toner M, Bacon D, Moul J, Veerapandian B, Gilliland GL. The crystal packing of two different crystal forms of bovine ribonuclease A. *J Cryst Growth* 1991;110:119–130.
21. Demel SJ, Doscher MS, Martin PD, Rodier F, Edwards BFP. 1.6-Angstrom structure of a semisynthetic ribonuclease crystallized from aqueous-ethanol—comparison with crystals from salt-solutions and with ribonuclease-A from aqueous alcohol-solutions. *Acta Crystallogr D* 1995;51:1003–1012.
22. King MV. Crystalline forms of bovine pancreatic ribonuclease: techniques of preparation, unit cells, and space groups. *Acta Crystallogr* 1956;9:460–465.
23. King MV, Bello J, Pignataro EH, Harker D. Crystalline forms of bovine pancreatic ribonuclease: some new modifications. *Acta Crystallogr* 1962;15:144–147.
24. Fankuchen I. An x-ray and crystallographic study of ribonuclease. *J Gen Physiol* 1941;24:315–316.
25. Brayer GD, McPherson A. Preliminary diffraction data for crystals of ribonuclease-A and ribonuclease-B and their complexes with deoxy(Pa)4 and deoxy(Pa)6. *J Biol Chem* 1982;257:3359–3361.
26. Martin PD, Petsko GA, Tsernoglou D. New high pH forms of ribonuclease A and S. *J Mol Biol* 1976;108:265–269.
27. Fedorov AA, Joseph-McCarthy D, Fedorov E, Sirakova D, Graf I, Almo SC. Ionic interactions in crystalline bovine pancreatic ribonuclease A. *Biochemistry* 1996;35:15962–15979.
28. Sorber HA. Handbook of biochemistry: selected data for molecular biology. In: Weast RC, editor. CRC. Cleveland, OH: The Chemical Rubber Co.; 1970. p 1622.
29. Battistel E, Bianchi D, Rialdi G. Thermodynamics of immobilized ribonuclease-A. *Pure Appl Chem* 1991;63:1483–1490.
30. Prento P. Glutaraldehyde for electron-microscopy—a practical investigation of commercial glutaraldehydes and glutaraldehyde-storage conditions. *Histochem J* 1995;27:906–913.
31. Plant AL, Locasciobrown L, Haller W, Durst RA. Immobilization of binding-proteins on nonporous supports—comparison of protein loading, activity, and stability. *Appl Biochem Biotech* 1991;30: 83–98.
32. DePhillips P, Lenhoff AM. Pore size distributions of cation-exchange adsorbents determined by inverse size-exclusion chromatography. *J Chromatogr A* 2000;883:39–54.
33. Connolly ML. Molecular-surface triangulation. *J Appl Crystallogr* 1985;18:499–505.
34. Connolly ML. The molecular-surface package. *J Mol Graphics* 1993;11:139–143.
35. Creighton TE. Proteins: structures and molecular properties. New York: W.H. Freeman and Co.; 1993. p 507.
36. Otwinowski Z, Minor W. Processing of x-ray diffraction data collected in oscillation mode. *Methods Enzymol* 1997;276:307–326.
37. Tanford C, Hauenstein JD. Hydrogen ion equilibria of ribonuclease. *J Am Chem Soc* 1956;78:5287–5291.
38. Kuntz ID. Hydration of macromolecules. 3. Hydration of polypeptides. *J Am Chem Soc* 1971;93:514–516.
39. Takahashi D, Kubota Y, Kokai K, Izumi T, Hirata M, Kokufuta E. Effects of surface charge distribution of proteins in their complexation with polyelectrolytes in an aqueous salt-free system. *Langmuir* 2000;16:3133–3140.
40. Neal BL, Asthagiri D, Lenhoff AM. Molecular origins of osmotic second virial coefficients of proteins. *Biophys J* 1998;75:2469–2477.
41. Curtis RA, Prausnitz JM, Blanch HW. Protein-protein and protein-salt interactions in aqueous protein solutions containing concentrated electrolytes. *Biotechnol Bioeng* 1998;57:11–21.
42. Ries-Kautt MM, Ducruix AF. Relative effectiveness of various ions on the solubility and crystal growth of lysozyme. *J Biol Chem* 1989;264:745–748.
43. Hofmeister F. Zur Lehre von der Wirkung der Salze. *Arch Exp Pathol Pharmacol* 1888;24:247–260.
44. Carbonnaux C, Ries-Kautt M, Ducruix A. Relative effectiveness of various anions on the solubility of acidic hypoderma-lineatum collagenase at pH 7.2. *Protein Sci* 1995;4:2123–2128.
45. Boyer M, Roy M, Jullien M, Bonneté F, Tardieu A. Protein interactions in concentrated ribonuclease solutions. *J Cryst Growth* 1999;196:185–192.
46. Russel WB, Saville DA, Schowalter WR. Colloidal dispersions. Cambridge: Cambridge University Press; 1989. p 525.
47. Mirarefi AM, Zukoski CF. Developing rapid screening methods and structural studies for soluble macromolecules. Paper presented at 75th ACS Colloid and Surface Science Symposium. 2001. Pittsburgh.
48. Kulkarni AM, Chatterjee AP, Schweizer KS, Zukoski CF. Effects of polyethylene glycol on protein interactions. *J Chem Phys* 2000;113:9863–9873.
49. Kulkarni AM, Chatterjee AP, Schweizer KS, Zukoski CF. Depletion interactions in the protein limit: effects of polymer density fluctuations. *Phys Rev Lett* 1999;83:4554–4557.
50. Chakrabarti P. Anion-binding sites in protein structures. *J Mol Biol* 1993;234:463–482.